



ARTICLE

## Static Analysis and Safety Assessment of Tilted Circular Sinking Wells

Anna Szymczak-Graczyk<sup>1,\*</sup>, Tomasz Garbowski<sup>2</sup>, Florim Grajčevci<sup>3</sup> and Hajdar Sadiku<sup>3</sup>

<sup>1</sup>Department of Construction and Geoen지니어ing, Faculty of Environmental and Mechanical Engineering, Poznan University of Life Sciences, Poznan, Poland

<sup>2</sup>Department of Biosystem Engineering, Faculty of Environmental and Mechanical Engineering, Poznan University of Life Sciences, Poznan, Poland

<sup>3</sup>Department of Construction, Faculty of Civil Engineering, University of Prishtina, Prishtina, Kosovo

\*Corresponding Author: Anna Szymczak-Graczyk. Email: [anna.szymczak-graczyk@up.poznan.pl](mailto:anna.szymczak-graczyk@up.poznan.pl)

Received: 17 January 2026; Accepted: 27 March 2026; Published: 30 June 2026

**ABSTRACT:** Sinking wells (open caissons) are widely used deep foundation structures whose installation by the cut-and-sink method may lead to unintended deviation from verticality due to heterogeneous soil conditions and construction irregularities. While tilting is a frequently observed phenomenon, quantitative criteria for assessing the admissibility of an inclined well after completion of sinking remain insufficiently defined. This study presents a static analytical framework for evaluating stress redistribution beneath the concrete plug of a tilted well. The analysis is based on eccentric vertical load transfer and derives closed-form relationships linking the permissible inclination angle to well geometry (radius  $r$ , height  $H$ ) and the ratio of total weight to shaft weight ( $G_c/G$ ). A practical admissibility criterion is proposed by limiting the increase in maximum contact stress to 20% relative to the vertical configuration ( $\sigma_1 \leq 1.2\sigma$ ). Parametric calculations performed for typical well dimensions ( $r = 2\text{--}5$  m,  $H = 4\text{--}9$  m) indicate that admissible inclination angles vary approximately from  $1.6^\circ$  to  $11.6^\circ$ , depending on geometric proportions and load distribution. The results demonstrate that stress amplification is governed primarily by bending moment induced by eccentricity rather than by axial load increase. The proposed formulation provides a transparent engineering tool enabling rapid assessment of whether a tilted sinking well may remain in service without exceeding acceptable soil stress amplification.

**KEYWORDS:** Sinking well; structural tilt; geotechnical design; soil stress; construction monitoring; cut-and-sink

### 1 Introduction

Sinking wells (open caissons) belong to a group of underground structures widely used in general, hydraulic, industrial, and environmental engineering, particularly under difficult soil–water conditions and where construction space is limited. This technology enables the construction of structures with significant foundation depths without the need for extensive excavation works or groundwater table lowering, which is of considerable technical and economic importance [1,2]. A sinking well is a reinforced concrete structure, most commonly with a circular or rectangular cross-section, equipped with a cutting edge that allows its gradual penetration into the ground under self-weight while the soil is excavated from its interior.

During construction, significant changes occur in the static structural scheme, ranging from a tubular system with free edges during the sinking phase to a tank supported along its perimeter after the execution of the concrete plug and bottom slab. This variability necessitates consideration of staged construction and three-dimensional structural behavior in static analysis and design [1–3].

Under ideal conditions, a circular sinking well may be treated as a thick-walled cylindrical shell subjected primarily to compressive stresses, allowing the application of classical plate and shell theory solutions [4]. Similar assumptions are commonly adopted in the analysis of cylindrical tanks founded on soil [5,6]. In practical construction, however, disturbances in the sinking process frequently occur due to soil heterogeneity, uneven excavation beneath the cutting edge, local obstacles in the ground, or asymmetric loads acting on the structure [1,3].

One of the most frequently observed and structurally significant phenomena accompanying the construction of sinking wells is the inclination of the well shaft from the vertical direction. This issue has been reported in studies on the design and construction of sinking wells, which emphasize the difficulty of correcting the structure's position at advanced stages of installation [1–3]. Such inclination leads to additional bending effects and alters the interaction conditions between the structure and the surrounding soil.

The importance of inclination as a key adverse effect is also confirmed by contemporary studies addressing construction risks during well sinking. Multicriteria analyses indicate that deviation from verticality is among the most frequent and critical hazards in the construction process, alongside excessive soil settlement and jamming of the well shaft within the ground [7].

Inclination of a sinking well significantly alters its static behavior, particularly the manner in which loads are transferred to the soil. In a vertical well, the load transmitted through the concrete plug is axial and approximately uniformly distributed. In contrast, an inclined well is subjected to eccentric loading, generating bending moments and a non-uniform stress distribution in the soil. The interaction between cylindrical structures and soil has been widely investigated in the literature, both within linear and nonlinear frameworks [8–11].

Research indicates that under eccentric loading of cylindrical structures, the adopted soil model and the selected soil strength criterion have a substantial influence on stress distribution [12–14]. Simplified elastic models may lead to underestimation of local stress concentrations, which directly affects the assessment of load-bearing capacity and operational safety. Non-uniform stress distributions may also initiate local limit states, including cracking or loss of stability of shell elements [15–17].

Inclination during the sinking process most commonly results from uneven excavation of soil from inside the well, the presence of local obstacles beneath the cutting edge, such as boulders or tree roots, heterogeneous soil layers often arranged with an inclination, as well as uneven surface loading around the well [1–3]. Similar causes of inclination are observed during the sinking of large-diameter open caissons, where asymmetry in earthworks and local ground disturbances lead to progressive deviations from verticality [18,19].

If inclination occurs during the sinking process, then after detecting elevation differences at the crown, it is often possible to restore the vertical position of the well shaft at subsequent stages of installation by applying appropriate construction measures [1,2]. Early detection of inclination and continuous monitoring of verticality during sinking are of crucial importance [19]. In practice, corrective actions applied during well straightening typically include the following methods:

- intensified excavation beneath the cutting edge on the side descending more slowly,
- increasing surface loading on the side descending more rapidly while simultaneously reducing ground level on the opposite side,
- additional loading of the well crown on the side exhibiting smaller settlement during continued sinking,
- local loosening of soil beneath the cutting edge at the location of slower descent, for example using high-pressure water jets [1–3,18].

A different situation arises when inclination develops after the well has reached its designed foundation depth. Such inclination may occur prior to the execution of the concrete plug, for example due to accidental impact on the upper part of the well shaft by construction equipment or as a result of uneven surface loading around an already sunk well [1–3]. In sinking wells constructed with a stepped cutting edge, a gap or zone of significantly loosened soil forms around the shaft above the step, which substantially increases the susceptibility of the structure to inclination caused even by minor dynamic actions [18].

When assessing whether a well will continue to tilt, it should be taken into account that active earth pressure acts on one side of the shaft, whereas on the side of inclination, where the shaft bears against the soil, passive earth resistance develops, whose magnitude exceeds that of active pressure. This mechanism is also described in stability analyses of vertical shafts and caissons constructed in soft and cohesionless soils [20].

Despite the practical importance of the discussed issue, neither the available literature nor current design standards provide clear quantitative criteria for assessing the permissible inclination of a sinking well after completion of construction. Existing studies focus primarily on issues of sinkability, buoyancy stability, and general soil–structure interaction, while the problem of safe operation of an inclined well is addressed only fragmentarily or qualitatively [1–3,7,21].

The aim of this study is to perform a static analysis of an inclined sinking well and to formulate a criterion enabling assessment of the admissibility of its continued operation. The analysis focuses on the influence of eccentric load transfer through the concrete plug on stress distribution in the surrounding soil. As a limit condition, an allowable increase in soil stresses relative to those occurring in a vertically constructed well is adopted. Previous studies have extensively analyzed soil–structure interaction of cylindrical tanks and shafts under eccentric loading [8–17,22–28]. However, quantitative admissibility criteria for post-construction tilting of sinking wells remain insufficiently addressed. The present study extends these interaction analyses toward a decision-oriented framework for tilted wells.

## 2 Materials and Methods

The available literature does not provide information on the magnitude of inclination that may be considered acceptable for a sinking well. In order to address the question of an admissible inclination that can be accepted from a structural safety perspective, the authors adopted the assumption that, as a result of inclination, the stresses transmitted to the soil by the concrete plug ( $\sigma_1$ ) are treated as the governing safety indicator. The permissible tilt angle  $\alpha$  is determined by imposing the condition that the maximum contact stress under the plug does not exceed 20% of the reference stress obtained for a perfectly vertical well ( $\sigma$ ), i.e.,  $\sigma_1(\alpha) \leq 1.2\sigma$ .

The adopted 20% stress increase limit is introduced as a conservative engineering criterion corresponding to a serviceability-based safety margin. In practical geotechnical design, moderate increases in contact stresses are often acceptable provided that soil bearing capacity and settlement limits are not exceeded. Similar relative stress increase limits have been discussed in tank–soil interaction studies addressing eccentric loading conditions [16,25–30]. The present study adopts this value as a transparent and conservative reference level for admissibility assessment.

The proposed 20% limit is intended for soils operating within their serviceability range and below ultimate bearing capacity. For cohesionless soils such as sand and gravel, where stress redistribution remains relatively stable under moderate eccentricity, the 20% increase may be considered appropriate. For cohesive and highly compressible soils, particularly soft clays sensitive to stress concentration, a reduced admissible increase (e.g., 10%–15%) may be adopted at the designer's discretion, depending on geotechnical investigation results and safety requirements. The soil–plug contact is assumed to remain fully compressive within the

considered range of tilt angles. Therefore, tensile contact stresses are not permitted in the adopted stress distribution, and the presented results should be interpreted as valid within the regime where loss of contact does not occur.

The inclined well shaft, together with the concrete plug already executed in the inclined position and having a horizontal top surface, transfers to the ground an eccentric load instead of the originally uniform load corresponding to the vertical well configuration and producing stress  $\sigma$ . As a result, non-uniform stresses  $\sigma_{1,2}$  develop in the soil. The eccentric loading arises from the uniformly distributed load associated with the self-weight of the concrete plug and from the bending moment generated by the eccentric position of the resultant weight of the inclined well shaft together with the superstructure, relative to the axis passing through the center of gravity of the concrete plug. Fig. 1 illustrates the system of vertical forces acting in the inclined sinking well.

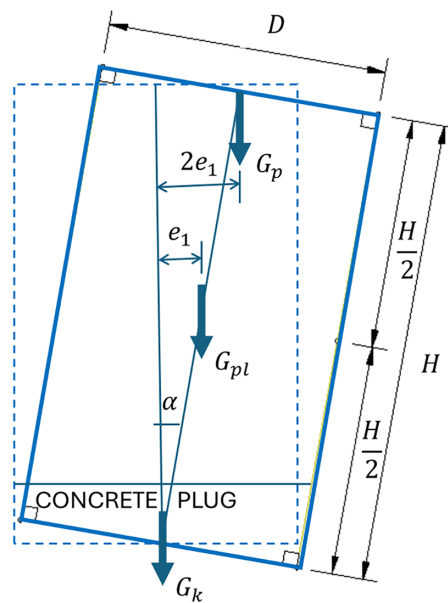


**Figure 1:** System of vertical forces acting in an inclined sinking well during installation.

Notation:

$H$ —height of the well shaft,

$D$ —external diameter of the well,

$G_k$ —weight of the concrete bottom-sealing plug (bottom-sealing concrete executed after reaching foundation depth)  $G_{pl}$ —weight of the well shaft,

$G_p$ —weight of the covering slab together with the soil placed on the slab,

$e_1$ —eccentricity of the line of action of the well shaft weight  $G_{pl}$  with respect to the center of gravity of the concrete plug; the weight  $G_p$  acts with an eccentricity of  $2e_1$  relative to the center of gravity of the concrete plug,

$\alpha$ —angle of inclination of the well from the vertical.

With the above notation, the following relationship is obtained:

$$\tan \alpha = \frac{e_1}{0.5H} = \frac{2e_1}{H}. \quad (1)$$

Denoting by  $e$  the eccentricity of the resultant force of  $G_{pl}$  and  $G_p$  (where  $G_{pl} + G_p = G$ ) and using the relationships shown in Fig. 1, one may write:

$$Ge = G_{pl}e_1 + G_p2e_1, \quad (2)$$

which gives:

$$e = \frac{G_{pl}e_1 + 2G_p e_1}{G} = \frac{e_1}{G} (G_{pl} + 2G_p). \quad (3)$$

Assuming that  $G_{pl} = G_p$  (i.e., the weight of the well shaft is equal to the weight of the covering slab together with the soil placed on it), Eq. (2) yields an eccentricity =  $1.5e_1$ , and the point of application of the resultant force  $G$  is then located at a height of  $0.75H$ . The tangent of the inclination angle  $\alpha$  is therefore:

$$\tan \alpha = \frac{1.5e_1}{0.75H} = \frac{2e_1}{H}. \quad (4)$$

The equality  $G_{pl} = G_p$  is introduced solely for illustrative simplification of the geometric relationship between eccentricity and inclination angle. The general formulation given in Eq. (3) remains valid for arbitrary weight ratios and may be applied directly when the shaft and superstructure weights differ. The admissible eccentricity relationships derived in Section 3 are expressed in terms of the ratio  $G_c/G$  and therefore remain applicable without imposing  $G_{pl} = G_p$ . This assumption is conservative in many practical configurations where the shaft weight may exceed the superstructure-related permanent load.

Knowing  $\tan \alpha$ , the inclination angle of the well may be calculated as:

$$\alpha = \arctan (\tan \alpha). \quad (5)$$

It should be emphasized that the force system illustrated in Fig. 1 represents only vertical load transfer mechanisms. The present analytical formulation does not explicitly model changes in lateral earth pressure acting on the well shaft due to tilting. Redistribution between active and passive earth pressure is discussed qualitatively in Section 1; however, the quantitative analysis is intentionally restricted to vertical stress amplification beneath the concrete plug. This assumption allows derivation of closed-form relationships and reflects the dominant mechanism governing foundation safety after completion of sinking. Shaft friction effects are therefore not explicitly included in the present closed-form model.

In practical engineering conditions, the shaft of a fully sunk caisson is subjected not only to vertical loading but also to lateral frictional resistance mobilized along the soil–structure interface. This effect reduces the portion of the caisson self-weight that is effectively transferred to the base. In the present analytical formulation, this phenomenon may be represented by introducing a reduction coefficient  $\eta$  applied to the shaft weight. The effective vertical load can therefore be written as  $G_{pl}^* = \eta G_{pl}$  where  $G_{pl}$  denotes the total weight of the caisson shaft and  $\eta$  is a dimensionless coefficient accounting for lateral friction along the caisson wall. The value of  $\eta$  depends on several factors, including soil type, groundwater conditions, interface roughness, and the construction history of the sinking process. In the present study, the coefficient is conservatively taken as  $\eta = 1$ , which corresponds to neglecting the contribution of lateral friction. This assumption allows the analytical model to remain transparent while preserving the possibility of incorporating the effect in future extensions of the framework.

The analysis is purely static and geometric. The load state is represented by the total permanent vertical loads acting on the well, including self-weight of structural elements and any additional permanent superstructure loads transmitted to the well during construction or service. These loads are collectively

denoted as  $G_c$ . Their ratio  $G_c/G$  is treated as the primary nondimensional parameter, allowing the results to be generalized across different well sizes and construction variants without introducing additional material-dependent assumptions. For a vertically positioned well, without inclination, the weights of the concrete plug  $G_k$ , the well shaft  $G_{pl}$ , and the covering slab  $G_p$  act along a common axis and produce a uniformly distributed soil reaction beneath the plug:

$$\sigma = \frac{G_k + G_{pl} + G_p}{F} = \frac{G_c}{F}, \quad (6)$$

where:

$G_c$ —total weight of the well,  $G_c = G_k + G_{pl} + G_p$ ,

$F$ —area of the concrete plug (e.g., for a well with external diameter  $D$ ,  $F = 0.25\pi D^2$ ).

For an inclined well, the stresses transmitted to the soil by the concrete plug are given by:

$$\sigma_{1,2} = \frac{G_c}{F} \pm \frac{\sum M_{ix}}{W_x}, \quad (7)$$

where  $\sum M_{ix}$  is defined by Eq. (2) thus:

$$\sigma_{1,2} = \frac{G_c}{F} \pm \frac{Ge}{W_x}. \quad (8)$$

For a circular cross-section, the section modulus is:

$$W_x = \frac{\pi r^3}{4} = \frac{\pi D^3}{32}, \quad (9)$$

where:  $r$ —radius of the concrete plug.

In water-bearing ground conditions, buoyancy effects may reduce the effective vertical loads transmitted to the soil. In such cases, the effective submerged weights of structural components should be used in the calculation of  $G$  and  $G_c$ . The present formulation therefore remains applicable provided that hydrostatic uplift is properly reflected in the adopted vertical load values.

Fig. 2 presents the distribution of stresses transmitted to the ground for a vertically positioned well (see Fig. 2a) and for a well inclined from the vertical (see Fig. 2b). The analysis assumes that the concrete plug is cast after the well has reached foundation depth and that its upper surface is horizontal, consistent with common construction practice. If the plug were cast with an inclined top surface matching the shaft inclination, the resultant eccentricity at the base would differ. Such a scenario would modify the stress distribution and lies beyond the scope of the present simplified formulation.

Taking into account the adopted assumption  $\sigma_1 \leq 1.2\sigma$ , it is necessary to determine the eccentricity  $e$  of the line of action of the resultant load  $G_{pl} + G_p$  (i.e., the weight of the well shaft and the covering slab, see Fig. 3) that, for an inclined well, will cause the maximum pressure on the soil beneath the concrete plug to increase by no more than 20%.

The force system generated by the self-weight of the well shaft and the covering slab is presented below, together with the corresponding eccentricities with respect to the axis passing through the center of gravity of the concrete plug. Calculations were also carried out to determine the admissible value of the eccentricity  $e$  that satisfies the adopted assumption.

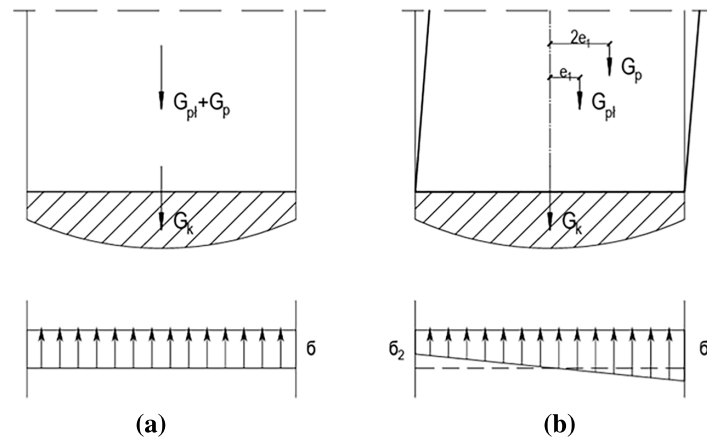


**Figure 2:** Stress distribution in the soil beneath the bottom plug: (a) for a vertical well and (b) for an inclined well.

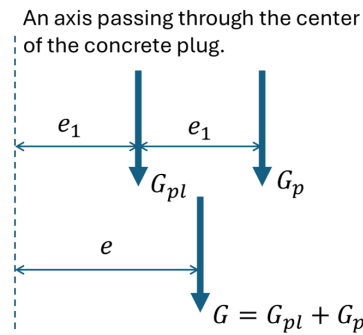


**Figure 3:** System of forces induced by the self-weight of the well shaft and the covering slab.

Based on the notation shown in Fig. 1 and relationships (1)–(9), calculations were performed under the adopted assumption  $\sigma_1 - \sigma = 0.2\sigma$ , i.e., a 20% increase in stresses. This increase is attributed to the bending moment generated by the weight of the inclined well shaft together with the superstructure, such that:

$$\frac{\sigma}{5} = \frac{M_x}{W_x}. \quad (10)$$

By consecutively combining the above relationships, Eq. (11) is obtained:

$$\sigma_1 - \sigma = \frac{M_x}{W_x} = \frac{4Ge}{\pi r^3} \rightarrow \frac{\sigma}{5} = \frac{4Ge}{\pi r^3} \rightarrow \frac{G_c}{5\pi r^2} = \frac{4Ge}{\pi r^3} \rightarrow e = \frac{G_c}{G} \frac{r}{20}. \quad (11)$$

The present formulation considers global equilibrium of vertical forces and bending moments transmitted to the soil beneath the plug. Shear stresses developing along the interface between the concrete plug and the well shaft are not explicitly evaluated. For the considered load case, these interface shear stresses are internal to the structural system and do not directly influence the maximum contact pressure beneath the base, which governs the adopted admissibility criterion. Their inclusion would require a detailed three-dimensional structural model and lies beyond the scope of the simplified analytical approach proposed herein.

### 3 Results

The analytical derivation presented herein is formulated for circular open caissons. The expressions for base area, section modulus and stress distribution correspond to circular geometry. For rectangular or special-shaped caissons, the general equilibrium relationship  $\sigma = N/F \pm M/W$  remains applicable; however, the base area  $F$  and section modulus  $W$  must be determined according to the specific cross-sectional geometry. In particular, rectangular caissons may exhibit local stress concentration near corners, which is not captured by the present formulation.

The analyzed object represents an idealized circular reinforced concrete sinking well with a rigid concrete bottom plug fully bonded to the shaft. The soil beneath the plug is modeled as a linear-elastic, homogeneous medium providing compressive reaction only. The shaft is assumed geometrically rigid for the purpose of global equilibrium evaluation. The adopted model corresponds to a completed well at foundation depth, after execution of the bottom plug.

The static analysis of the inclined open caisson was performed using the model described in [Section 2](#). The results presented below correspond to systematic parametric calculations rather than a single site-specific case study.

Using [Eq. \(11\)](#), the admissible values of the eccentricity  $e$  were determined as a function of the weights of the individual well components and the radius of the concrete plug, under the condition derived from the assumption  $\sigma_1 \leq 1.2\sigma$ . The calculated results are summarized in [Table 1](#).

**Table 1:** Admissible eccentricity  $e$  of the resultant gravity load as a function of the ratio  $G_c/G$  and the well radius  $r$ , satisfying the condition  $\sigma_1 \leq 1.2\sigma$ .

$G_c/G$	1.25	1.35	1.50	1.65
$e$ ( <a href="#">Eq. (11)</a> )	$0.0625r$	$0.0675r$	$0.075r$	$0.0825r$

For a circular cross-section, absence of tensile contact stresses requires that the eccentricity remains within the kern, i.e.,  $e \leq r/4$ . From [Eq. \(11\)](#), the maximum eccentricity considered in this study equals  $e = (G_c/G)r/20$ . For the highest analyzed ratio  $G_c/G = 1.65$ , this yields  $e = 0.0825r$ , which satisfies  $e < r/4$ . Therefore, all tabulated admissible inclination values remain within the compressive contact regime assumed in the analysis.

Assuming that the well remains open at the top ( $G_p = 0$ ), it follows that  $G = G_{pl}$ . In this case, the eccentricity is  $e = e_1$ , and the center of gravity of the well shaft is located at a height of  $0.5H$ . Consequently, the tangent of the inclination angle is given by

$$\tan \alpha = \frac{e_1}{0.5H} = \frac{2e_1}{H}. \quad (12)$$

The obtained results are presented in [Table 2](#) and are identical to those listed in [Table 1](#). Additionally, relationships are provided that enable the determination of  $\tan \alpha$  for wells with a given radius  $r$  and shaft height  $H$ , for different ratios of the weights of the individual well components.

Using the relationships presented in [Tables 1](#) and [2](#), admissible values of the well shaft inclination angle  $\alpha$  are calculated for selected example wells, for which the adopted assumption is satisfied that the increase in soil stresses beneath the concrete plug does not exceed 20% of the stresses that would occur for a vertically positioned well. The calculation results are summarized in [Tables 3–6](#), which refers to wells with a weight ratio  $G_c/G = 1.25, 1.35, 1.50, 1.65$ . The results summarized in [Tables 3–6](#) indicate a clear reduction of the

permissible tilt angle with increasing shaft height  $H$ . For a fixed  $H$ , larger well sizes (higher  $r$  or  $D$ ) generally correspond to smaller admissible  $\alpha$  values, reflecting the higher sensitivity of contact stresses to eccentric loading in larger foundations. Moreover, increasing the plug-to-shaft weight ratio  $G_c/G$  consistently reduces the allowable inclination, as the plug contributes directly to the stress amplification beneath the base.

**Table 2:** Relationships for the tangent of the admissible inclination angle  $\alpha$  of the well shaft, satisfying  $\sigma_1 \leq 1.2\sigma$ , as a function of the ratios  $G_c/G$ , the well radius  $r$ , and the shaft height  $H$ .

$G_c/G$	1.25	1.35	1.50	1.65
$e_1$ (Eq. (11))	$0.0625r$	$0.0675r$	$0.075r$	$0.0825r$
$\tan \alpha$	$0.125r/H$	$0.135r/H$	$0.150r/H$	$0.165r/H$

**Table 3:** Admissible values of the well inclination angle  $\alpha$  satisfying  $\sigma_1 \leq 1.2\sigma$  for  $G_c/G = 1.25$ , as a function of the well radius  $r$  and the shaft height  $H$ .

Well Height $H$ [m]	Well Radius $r$ [m]							
	2		3		4		5	
	$\tan \alpha$	$\alpha$ [deg]	$\tan \alpha$	$\alpha$ [deg]	$\tan \alpha$	$\alpha$ [deg]	$\tan \alpha$	$\alpha$ [deg]
4	0.063	3.58	0.094	5.36	0.125	7.13	0.156	8.88
5	0.050	2.86	0.075	4.29	0.100	5.71	0.125	7.13
6	0.042	2.39	0.063	3.58	0.083	4.76	0.104	5.95
7	0.036	2.05	0.054	3.07	0.071	4.09	0.089	5.10
8	0.031	1.79	0.047	2.68	0.063	3.58	0.078	4.47
9	0.028	1.59	0.042	2.39	0.056	3.18	0.069	3.97

**Table 4:** Admissible values of the well inclination angle  $\alpha$  satisfying  $\sigma_1 \leq 1.2\sigma$  for  $G_c/G = 1.35$ , as a function of the well radius  $r$  and the shaft height  $H$ .

Well Height $H$ [m]	Well Radius $r$ [m]							
	2		3		4		5	
	$\tan \alpha$	$\alpha$ [deg]	$\tan \alpha$	$\alpha$ [deg]	$\tan \alpha$	$\alpha$ [deg]	$\tan \alpha$	$\alpha$ [deg]
4	0.068	3.86	0.101	5.78	0.135	7.69	0.169	9.58
5	0.054	3.09	0.061	4.63	0.108	6.16	0.135	7.69
6	0.045	2.58	0.068	3.86	0.090	5.14	0.113	6.42
7	0.039	2.21	0.058	3.31	0.077	4.41	0.096	5.51
8	0.034	1.93	0.051	2.90	0.068	3.86	0.084	4.82
9	0.030	1.72	0.045	2.58	0.060	3.43	0.075	4.29

During the construction of the well, the correctness of its sinking is controlled by means of geodetic measurements of elevation levels taken at several points on the crown of the well. Tables 7–10 present the permissible differences in the measured elevation levels on the well crown for selected well parameters ( $G_c/G$ ,  $H$  and  $D$ ). These values were calculated on the basis of the permissible angles of deviation of the well axis from the vertical, as given in Tables 3–6. A direct comparison between the cases with and without the concrete plug (Tables 3–6 vs. Tables 7–10) shows that removing the plug substantially increases the permissible tilt angle.

This effect becomes particularly pronounced for larger wells and for taller shafts, where the stress increase induced by eccentricity is more severe when the plug contributes additional concentrated loading at the base.

**Table 5:** Admissible values of the well inclination angle  $\alpha$  satisfying  $\sigma_1 \leq 1.2\sigma$  for  $G_c/G = 1.50$ , as a function of the well radius  $r$  and the shaft height  $H$ .

Well Height $H$ [m]	Well Radius $r$ [m]							
	2		3		4		5	
	$\tan \alpha$	$\alpha$ [deg]	$\tan \alpha$	$\alpha$ [deg]	$\tan \alpha$	$\alpha$ [deg]	$\tan \alpha$	$\alpha$ [deg]
4	0.075	4.29	0.113	6.42	0.150	8.53	0.188	10.62
5	0.060	3.43	0.090	5.14	0.120	6.84	0.150	8.53
6	0.050	2.86	0.075	4.29	0.100	5.71	0.125	7.13
7	0.043	2.45	0.064	3.68	0.086	4.90	0.107	6.12
8	0.038	2.15	0.056	3.22	0.075	4.29	0.094	5.36
9	0.033	1.91	0.050	2.86	0.067	3.81	0.083	4.76

**Table 6:** Admissible values of the well inclination angle  $\alpha$  satisfying  $\sigma_1 \leq 1.2\sigma$  for  $G_c/G = 1.65$ , as a function of the well radius  $r$  and the shaft height  $H$ .

Well Height $H$ [m]	Well Radius $r$ [m]							
	2		3		4		5	
	$\tan \alpha$	$\alpha$ [deg]	$\tan \alpha$	$\alpha$ [deg]	$\tan \alpha$	$\alpha$ [deg]	$\tan \alpha$	$\alpha$ [deg]
4	0.083	4.72	0.124	7.05	0.165	9.37	0.206	11.65
5	0.066	3.78	0.099	5.65	0.132	7.52	0.165	9.37
6	0.055	3.15	0.083	4.72	0.110	6.28	0.138	7.83
7	0.047	2.70	0.071	4.04	0.094	5.39	0.118	6.72
8	0.041	2.36	0.062	3.54	0.083	4.72	0.103	5.89
9	0.037	2.10	0.055	3.15	0.073	4.19	0.092	5.24

**Table 7:** Permissible crown height difference  $h$  (cm) ensuring  $\sigma_1 < 1.2\sigma$  vs. well diameter  $D$  and lining height  $H$ , for  $G_c/G = 1.25$ .

Well Height $H$ [m]	Well Diameter $D$ [m]			
	3	4	6	8
	$h$ [cm]			
4	14.1	25.0	56.3	100.0
5	11.3	20.0	45.0	80.0
6	9.4	16.7	37.5	66.7
7	8.0	14.3	32.1	57.1
8	7.0	12.5	28.1	50.0
9	6.25	11.1	25.0	44.4

**Table 8:** Permissible crown height difference  $h$  (cm) ensuring  $\sigma_1 < 1.2\sigma$  vs. well diameter  $D$  and lining height  $H$ , for  $G_c/G = 1.35$ .

Well Height $H$ [m]	Well Diameter $D$ [m]			
	3	4	6	8
	$h$ [cm]			
4	15.2	27.0	60.7	108.0
5	12.2	21.6	48.6	86.3
6	10.1	18.0	40.5	72.0
7	8.7	15.4	34.7	61.7
8	7.6	13.5	30.4	54.0
9	6.8	12.0	27.0	48.0

**Table 9:** Permissible crown height difference  $h$  (cm) ensuring  $\sigma_1 < 1.2\sigma$  vs. well diameter  $D$  and lining height  $H$ , for  $G_c/G = 1.50$ .

Well Height $H$ [m]	Well Diameter $D$ [m]			
	3	4	6	8
	$h$ [cm]			
4	16.9	30.0	67.5	120.0
5	13.5	24.0	54.0	96.0
6	11.3	20.0	45.0	80.0
7	9.6	17.1	38.6	68.6
8	8.4	15.0	33.8	60.0
9	7.5	13.3	30.0	53.3

**Table 10:** Permissible crown height difference  $h$  (cm) ensuring  $\sigma_1 < 1.2\sigma$  vs. well diameter  $D$  and lining height  $H$ , for  $G_c/G = 1.65$ .

Well Height $H$ [m]	Well Diameter $D$ [m]			
	3	4	6	8
	$h$ [cm]			
4	18.6	33.0	74.2	132.0
5	14.8	26.4	59.4	105.6
6	12.4	22.0	49.5	88.0
7	10.6	18.9	42.4	75.5
8	9.3	16.5	37.1	66.1
9	8.3	14.7	33.0	58.7

Inspection of the analytical relationships indicates that the admissible inclination angle scales approximately with the ratio  $r/H$  and inversely with the weight ratio  $G_c/G$ . The shaft height  $H$  exerts the strongest influence on permissible tilt due to its direct role in eccentricity amplification ( $\tan \alpha \propto e/H$ ), whereas the

radius  $r$  primarily affects stress redistribution through the section modulus term. The weight ratio  $G_c/G$  governs the magnitude of stress amplification for a given eccentricity. Among these parameters, shaft height  $H$  exhibits the highest sensitivity in practical design ranges.

If the measured values of  $h$  are smaller than those given in Tables 7–10, this indicates that the inclination angle of the well is smaller than the value considered permissible, provided that the condition  $\sigma_1 < 1.2\sigma$  is satisfied (Fig. 4).

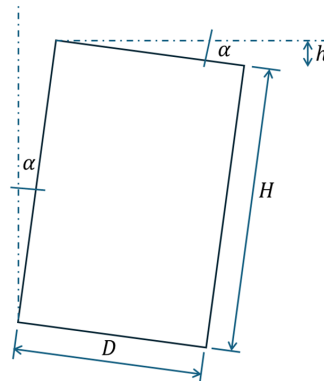


**Figure 4:** Determination of the inclination angle  $\alpha$  of the well from the measured height difference  $h$  on the well crown.

Tables 7–10 present the permissible height differences  $h$  (cm) between points on the crown of the well lining tilted by an angle  $\alpha$ , as specified in Tables 3–6.

In contemporary structural health monitoring practice, inclination of underground structures may be measured not only by geodetic crown elevation differences but also by inclinometers, tiltmeters, fiber optic sensing systems, and satellite-based InSAR techniques. These technologies provide continuous or high-resolution tilt measurements that can be directly integrated with the proposed analytical framework by converting measured angular deviation into equivalent eccentricity and contact stress amplification. The presented criterion therefore complements modern monitoring systems by providing a quantitative interpretation of measured tilt values in terms of foundation stress state.

Fig. 5 presents maps of the permissible well inclination angle  $\alpha$  as a function of the well radius  $r$  and lining height  $H$ , ensuring the stress criterion  $\sigma_1 < 1.2\sigma$ . Subfigures (a–d) correspond to different ratios  $G_c/G$ , ranging from 1.25 to 1.65.

When using the values given in Tables 3–6 for the well deviation angle  $\alpha_0$  from the vertical and in Tables 7–10 for the height difference  $h$  (cm) between points measured on the well crown, the corresponding values for intermediate parameters  $H$ ,  $D$  and  $G_c/G$  may be calculated by interpolation.

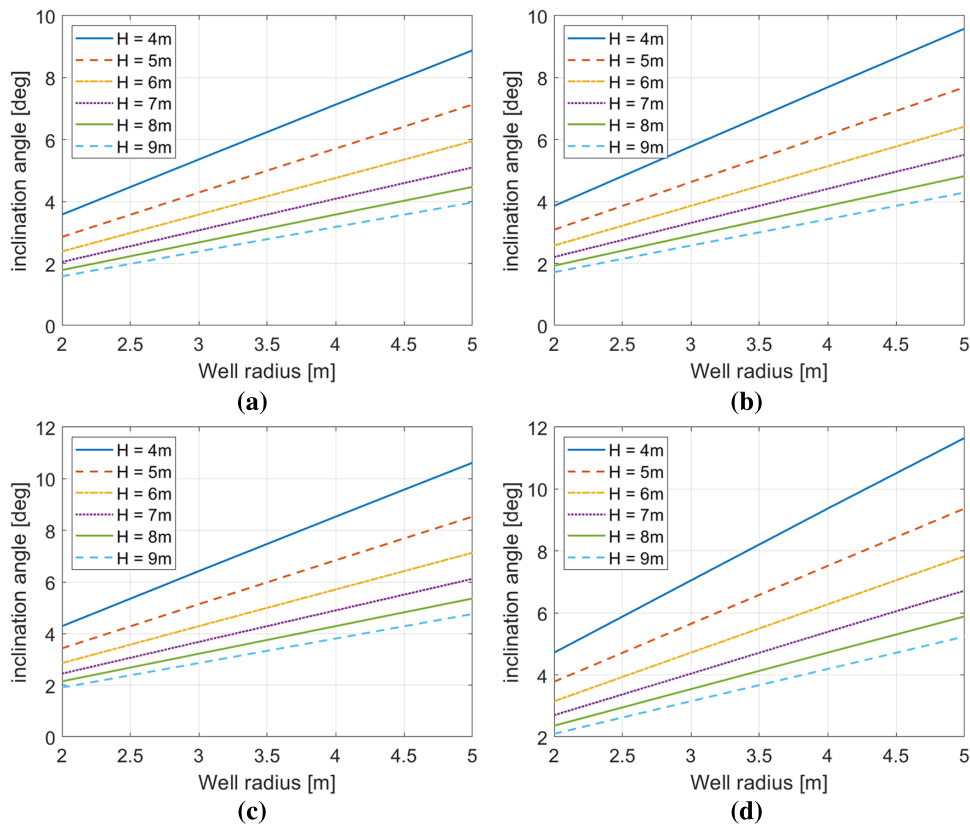


**Figure 5:** Plots of permissible well inclination  $\alpha$  vs. radius  $r$  and lining height  $H$  for  $\sigma_1 < 1.2\sigma$ : (a)  $G_c/G = 1.25$ ; (b) 1.35; (c) 1.50; (d) 1.65.

#### 4 Discussion

The results of the static analysis of the tilted sinking well confirm that even a small deviation of the structure's axis from the vertical leads to a significant change in the pattern of load transfer to the ground. In the case of a vertical well, the distribution of contact stresses under the concrete plug is approximately uniform, whereas tilting of the structure causes a linearly varying stress distribution with a pronounced concentration on the side of the deviation. Similar stress redistribution mechanisms have been reported in studies on the interaction of cylindrical reinforced concrete tanks with the soil foundation, where eccentric loading results in asymmetric base pressure [8,9].

According to the presented results, the decisive factor responsible for the increase in maximum contact stresses is the bending moment induced by the eccentric position of the resultant vertical loads, rather than the increase in normal force itself. This mode of structural behavior is consistent with observations reported in studies [8–10,16,17], which demonstrated that bending moments generated by geometric or thermal effects may have a greater influence on the stress state of the foundation than axial loads [10,16].

The analysis of the relationship between the tilt angle and the maximum contact stresses revealed a quasi-linear increase in stresses for small tilt angles, with acceleration for larger deviations from vertical. A similar behavior has been observed in analyses of cylindrical tanks and silos with variable wall thickness, where increasing eccentricity leads to a nonlinear redistribution of stresses in the soil foundation [22,23]. The results of the present study extend these observations to sinking well structures, where the bending moment arises as a result of tilting rather than external loading.

An important finding is that for the considered parameter range, contact between the base of the concrete plug and the soil is expected. This phenomenon is consistent with conclusions from studies on cylindrical tanks and foundations, which emphasized that asymmetric base pressure does not necessarily lead to detachment of the base but may result in local soil overloading [5,24]. In this context, the present study confirms the validity of assessing the safety of a tilted well based on the increase in contact stresses, rather than solely on geometric criteria. The influence of lateral friction along the caisson wall may reduce the effective vertical load transmitted to the base; however, due to the large uncertainty associated with soil–structure interaction parameters, this effect was not explicitly quantified in the present study.

The tilt permissibility criterion proposed in this study, based on limiting the increase of maximum contact stresses to  $\sigma_1 \leq 1.2\sigma$ , represents an extension of approaches used in the safety analyses of tanks and reinforced concrete structures founded directly on soil. Similar stress increase limits have been considered in studies evaluating the influence of soil modeling on the safety of tank structures [16,25–27]; however, the literature lacks explicit criteria directly addressing tilting of sinking wells.

Comparison of the results for tilted and vertical wells confirms that the change in the structural load-bearing scheme is qualitative rather than merely quantitative. Even with identical vertical load values  $N$ , introducing a bending moment  $M$  results in a significant increase in maximum contact stresses. These conclusions are consistent with observations in vertical tanks and shafts, where eccentric loading leads to substantial changes in the operational conditions of the structure and the foundation [20,28].

It should be emphasized that the presented results are based on the adopted modeling assumptions, particularly the linear-elastic soil model and the absence of cracking in the reinforced concrete structure. As noted in studies on the nonlinear interaction of cylindrical structures with soil, considering soil plasticity may lead to partial redistribution of contact stresses [11,13]. Nevertheless, within the scope of engineering assessment for the usability of a tilted well, the proposed approach provides a practical and safe decision-making tool.

The applicability of the proposed stress increase criterion depends on soil mechanical properties. The present formulation assumes that the soil remains within its elastic or quasi-elastic response range. In soils characterized by low deformation modulus or high sensitivity to stress concentration (e.g., soft clay), a lower admissible stress amplification limit may be required. The framework proposed herein allows straightforward adjustment of the admissible percentage increase according to project-specific geotechnical conditions.

Furthermore, nonlinear numerical simulation considering full soil–structure interaction would enable evaluation of the deviation between the simplified analytical model and actual stress conditions. The present work intentionally prioritizes analytical transparency and closed-form applicability. Detailed finite element verification and potential calibration coefficients constitute a recommended direction for future investigation. In summary, the results of this study align with the existing body of research on the interaction of cylindrical structures with soil foundations while extending it to the problem of tilting in sinking wells, which has previously been addressed mainly qualitatively or from a construction perspective. The introduction of a quantitative tilt permissibility criterion, directly based on static analysis, represents a significant contribution to the development of methods for assessing the safety of this type of structure.

## 5 Conclusions

The conducted analysis confirms that inclination of a sinking well fundamentally alters the load transfer mechanism between the structure and the soil foundation. Even small deviations from verticality introduce eccentricity of vertical loads, generating bending moments that lead to non-uniform contact stress distribution beneath the concrete plug.

The study demonstrates that the increase in maximum contact stress is primarily controlled by the bending component associated with eccentricity rather than by an increase in axial force. This distinction is essential for rational safety assessment of tilted wells.

A quantitative admissibility criterion was proposed by limiting the maximum contact stress beneath the plug to 20% above the reference value for a vertical well. Closed-form relationships were derived linking permissible inclination to geometric parameters and weight ratios. The parametric evaluation indicates that the allowable tilt angle decreases with increasing shaft height and increasing contribution of plug weight to total load.

For typical engineering ranges of well dimensions, the admissible inclination varies within a limited interval, highlighting the sensitivity of larger and taller wells to eccentric loading effects. Extension of the proposed admissibility framework to non-circular caisson geometries, including rectangular and polygonal cross-sections, requires dedicated evaluation of section properties and potential corner stress concentration effects and constitutes a natural direction for further development.

The present analysis addresses immediate static stress redistribution after completion of construction. Time-dependent effects such as soil consolidation, creep under sustained eccentric loading, and cyclic loading influence long-term behavior and may modify contact stress evolution. Incorporation of such phenomena requires advanced constitutive modeling and represents an important extension of the current framework.

The present study is analytical in nature and aims at establishing transparent closed-form relationships for engineering assessment. Validation using monitored field cases, including comparison with measured inclination and soil stress data, represents an important continuation of this work and will enable further calibration of the proposed admissibility limits.

The proposed analytical framework provides a practical decision-support tool for evaluating post-construction inclination of sinking wells using measurable geometric parameters and crown elevation differences. Although based on simplified linear-elastic soil assumptions, the method offers a conservative and transparent basis for engineering judgment. Future research may extend the approach toward nonlinear soil modeling and three-dimensional numerical validation.

**Acknowledgement:** None.

**Funding Statement:** The authors received no specific funding for this study.

**Author Contributions:** The authors confirm contribution to the paper as follows: Conceptualization, Anna Szymczak-Graczyk; methodology, Anna Szymczak-Graczyk; software, Tomasz Garbowski; validation, Florim Grajčevci and Hajdar Sadiku; formal analysis, Anna Szymczak-Graczyk and Florim Grajčevci; investigation, Tomasz Garbowski and Hajdar Sadiku; resources, Hajdar Sadiku and Florim Grajčevci; data curation, Florim Grajčevci and Hajdar Sadiku; writing—original draft preparation, Anna Szymczak-Graczyk; writing—review and editing, Tomasz Garbowski; visualization, Anna Szymczak-Graczyk and Tomasz Garbowski; supervision, Anna Szymczak-Graczyk and Tomasz Garbowski; project administration, Anna Szymczak-Graczyk and Tomasz Garbowski; funding acquisition, Anna Szymczak-Graczyk. All authors reviewed and approved the final version of the manuscript.

**Availability of Data and Materials:** The data that support the findings of this study are available from the Corresponding Author, [Anna Szymczak-Graczyk], upon reasonable request.

**Ethics Approval:** Not applicable.

**Conflicts of Interest:** The authors declare no conflicts of interest.

## References

1. Szymczak-Graczyk A. Żelbetowe studnie opuszczane. Kształtowanie, obliczenia, wykonawstwo, przykłady realizacji [Reinforced concrete sunk wells: design, calculations, construction, case studies]. Poznań, Poland: Poznań University of Life Sciences Press; 2021. (In Polish).
2. Szymczak-Graczyk A. Selected aspects of the design and construction of reinforced concrete sunk wells. *Acta Sci Pol Archit.* 2022;21(3):43–54. doi:10.22630/aspa.2022.21.3.21.
3. Szymczak Graczyk A. Metody obliczania studni opuszczanych [Calculation methods for sunk wells]. *Przegl Bud.* 2024;95(4):91–4. doi:10.5604/01.3001.0054.6393.
4. Timoshenko SP, Woinowsky-Krieger S. *Theory of plates and shells.* 2nd ed. New York, NY, USA: McGraw Hill; 1987.
5. Silva RLC, Marques GB, Lages EN, Marques SPC. Analytical study of cylindrical tanks including soil-structure interaction. *Rev IBRACON Estrut Mater.* 2019;12(1):14–22. doi:10.1590/s1983-41952019000100003.
6. Rodd J, Castel A. Structural considerations to minimise the risk of horizontal cracks in the wall of circular concrete tanks. *Structures.* 2022;40(4):1091–106. doi:10.1016/j.istruc.2022.04.066.
7. Dachowski R, Gałek-Bracha K. Determination of the occurrence of negative impacts during lowering of sinking wells using the fuzzy TOPSIS method. *Sustainability.* 2024;16(2):899. doi:10.3390/su16020899.
8. Lewiński PM. *The analysis of the interaction of reinforced concrete cylindrical tanks with subsoil.* Warsaw, Poland: Building Research Institute (ITB); 2007.
9. Lewiński PM. Accuracy assessment of linear elasticity solution for interaction of cylindrical tank with subsoil. *Bull Pol Acad Sci Tech Sci.* 2021;136039. doi:10.24425/bpasts.2021.136039.
10. Lewiński PM. Interaction of RC and PC cylindrical silos and tanks with subsoil. *Arch Civ Eng.* 2020;66(4):249–67.
11. Lewiński PM, Dudziak S. Nonlinear interaction analysis of RC cylindrical tank with subsoil by adopting two kinds of constitutive models for ground and structure. *AIP Conf Proc.* 2018;1922:130007. doi:10.1063/1.5019137.
12. Wiłun Z. *Zarys geotechniki [Outline of geotechnics].* Warsaw, Poland: Transport and Communications Publishers; 2010. (In Polish).
13. Drucker DC, Prager W. Soil mechanics and plastic analysis or limit design. *Q Appl Math.* 1952;10(2):157–65. doi:10.1090/qam/48291.
14. Wojciechowski M. A note on the differences between Drucker-Prager and Mohr-Coulomb shear strength criteria. *Stud Geotech Mech.* 2018;40(3):163–9. doi:10.2478/sgem-2018-0016.
15. Marzec I, Bobiński J, Tejchman J, Schönngel J. Finite element analysis on failure of reinforced concrete corner in sewage tank under opening bending moment. *Eng Struct.* 2021;228(1):111506. doi:10.1016/j.engstruct.2020.111506.
16. Halicka A, Zięba J. Influence of the subsoil model on the safety and eco-efficiency of reinforced concrete structure of rectangular liquid tank founded beneath the terrain surface. *Eng Struct.* 2024;303(2):117571. doi:10.1016/j.engstruct.2024.117571.
17. Kawecki B, Halicka A, Podgórski J. Buckling of cylindrical concrete tanks and silos due to prestressing—nonlinear approach. *Thin Walled Struct.* 2022;176:109339. doi:10.1016/j.tws.2022.109339.
18. Abdrabbo F, Gaaver K. Challenges and uncertainties relating to open caissons. *J Deep Found Inst.* 2012;6(1):21–32. doi:10.1179/dfi.2012.002.
19. Royston R, Sheil BB, Byrne BW. Monitoring the construction of a large-diameter caisson in sand. *Proc Inst Civ Eng Geotech Eng.* 2022;175(3):323–39. doi:10.1680/jgeen.19.00266.
20. Wang J, Abbasi NS, Pan W, Alidekyi SN, Li H, Ahmed B, et al. A review of vertical shaft technology and application in soft soil for urban underground space. *Appl Sci.* 2025;15(6):3299. doi:10.3390/app15063299.
21. State of art report on well foundation—open sinking method. [cited 2026 Jan 1]. Available from: <https://www.scribd.com/document/811039007/STATE-OF-ART-REPORT-ON-WELL-FOUNDATION>.
22. Lewiński PM, Rak M. Soil-structure interaction of cylindrical tank of variable wall thickness under the constant thermal loading. *Arch Civ Eng.* 2020;66(4):269–85. doi:10.24425/ace.2020.135221.
23. Lewiński PM, Rak M. Soil-structure interaction of cylindrical tank of variable wall thickness under the thermal gradient conditions. *IOP Conf Ser Mater Sci Eng.* 2019;661(1):012044. doi:10.1088/1757-899X/661/1/012044.

24. Kliszczewicz B. The interaction of a reinforced concrete cylindrical tank with soil in complicated functional conditions. *E3S Web Conf.* 2018;45:00030. doi:10.1051/e3sconf/20184500030.
25. Gogolik S, Koprás M, Szymczak-Graczyk A, Tschuschke W. Experimental evaluation of the size and distribution of lateral pressure on the walls of the excavation support. *J Build Eng.* 2023;73:106831. doi:10.1016/j.jobe.2023.106831.
26. Omid Bidgoli M, Kashyzadeh KR, Rahimian Kolor SS, Petrů M, Amiri N. Optimum design of Sunken reinforced enclosures under buckling condition. *Appl Sci.* 2020;10(23):8449. doi:10.3390/app10238449.
27. Szymczak-Graczyk A. The effect of subgrade coefficient on static work of a pontoon made as a monolithic closed tank. *Appl Sci.* 2021;11(9):4259. doi:10.3390/app11094259.
28. Jones K, Sun M, Lin C. Integrated analysis of LNG tank superstructure and foundation under lateral loading. *Eng Struct.* 2022;253(11):113795. doi:10.1016/j.engstruct.2021.113795.
29. Garbowski T, Pawlak TG, Szymczak-Graczyk A. Efficient load-bearing capacity assessment of a degraded concrete manhole using sectional homogenization. *Materials.* 2024;17(23):5883. doi:10.3390/ma17235883.
30. Jiang BN, Wang MT, Chen T, Zhang LL, Ma JL. Experimental study on the migration regularity of sand outside a large, deep-water, open caisson during sinking. *Ocean Eng.* 2019;193(1):106601. doi:10.1016/j.oceaneng.2019.106601.